Heliyon 6 (2020) e04611

Contents lists available at ScienceDirect

Heliyon

journal homepage: www.cell.com/heliyon

Research article

Usage of shape memory alloy actuators for large force active disassembly applications

Hoda Abuzied [a,b,*], Ayman Abbas [a], Mohamed Awad [b], Hesham Senbel [b]

[a] Mechanical Engineering Department, Faculty of Engineering, The British University in Egypt (BUE), El Sherouk City, 11837, Cairo, Egypt
[b] Design & Production Engineering Department, Faculty of Engineering, Ain Shams University, Abbasseya, 11535, Cairo, Egypt

ARTICLE INFO

Keywords:
Materials science
Mechanical engineering
Manufacturing engineering
Machine design
Mechanical systems
Alloys
Strain
Active disassembly
Shape memory alloy
Compressive strain
Recovery force

ABSTRACT

Shape memory alloys (SMAs) possess inherent superior properties that make their applications in active disassembly an emerging and interesting field of research. This is because extremely large forces can be generated repeatedly using a small compact-sized element, such as an SMA actuator. To ensure the ability of the SMA actuator to generate a repeated large force or withstand repeated load, several factors should be considered. These include factors that affect the value of the generated recovery forces, such as the amount of strain used, activation temperature, activation time, and cross-sectional area of the SMA element. In general, the compressive strain can be considered as the most influential factor that affects the value of the generated recovery force. The present research investigates the possible use of the SMA actuator in large-force active disassembly applications. To the best of the authors' knowledge, all the studies conducted in this field are concerned with implementing active disassembly in applications requiring small disassembly forces. The present research was conducted in three phases. First, the behaviour of the SMA element upon exposure to different repetitive compressive strains was studied, and the generated recovery force and strain hardening induced in the material were considered to ensure the continuous generation of large recovery forces with the least amount of residual strain induced in the material. Second, the optimum value of the compressive strain required to generate the maximum force with the least amount of residual strain induced in the material was estimated. Third, a practical case study was presented to validate the possible implementation of SMA actuators in large force active disassembly applications. The study successfully estimated the optimum compressive strain value that generated the required recovery force to disassemble the conducted case study using active disassembly technique.

1. Introduction

Active disassembly (AD) is the process of inserting innovative components made of smart materials into a product during its design phase to enable the cost-effective and non-destructive self-separation of the product [1, 2]. This is attributed to the ability of smart materials to sense any change in the working environment along with their rapid multi-dimensional response [3]. Shape memory is a unique property of smart materials that enhances their ability to be used as sensors and actuators. This property enables a deformed material to recover its original shape upon application of a thermal or mechanical stimulus [4].

Shape memory alloys (SMAs) can be classified into two main types: heat activated and magnetic responsive. SMAs can be considered as one of the most common types of smart materials that can restore their original shape upon heating [5]. In addition to their ability to change their mechanical properties [6], SMAs can restore large deformations and produce large stresses upon exposure to a specific mechanical or thermal stimulus [7].

These behaviours are due to reversible martensitic phase transformation, which is responsible for the unique set of functional properties of SMAs, such as shape memory effect (SME) and pseudo elasticity [4, 8]. These properties promote SMAs over other types of smart materials as SME is responsible for restoring the original shape of the SMA element upon heating, while pseudo elasticity is responsible for recovering large amounts of strain (up to 8%) [9, 10]. In general, the induced strain hardening in a deformed SMA can be eliminated by heating it to a temperature higher than the austenite finish temperature [11, 12]. However, as overheating could harm the SMA element and reduce its expected lifetime, increasing the heating temperature above the recommended austenite finish temperature must be done in a controlled manner [13]. E.

* Corresponding author.
E-mail address: hoda.abuzied@bue.edu.eg (H. Abuzied).

https://doi.org/10.1016/j.heliyon.2020.e04611
Received 18 April 2020; Received in revised form 19 June 2020; Accepted 29 July 2020

Henderson et al. [12] recommended increasing the heating temperature used for testing nickel-titanium (NiTi) wires over the manufacturer's recommended austenite finish temperature by 20–40 °C. T. Fukuta et al. [14] recommended increasing the heating temperature used for testing NiTi round bars by up to 50 °C above the manufacturer's recommended austenite finish temperature. Thus, the induced residual strains due to repeated loading could be relieved by heating to a temperature 20–50 °C higher than the recommended austenite finish temperature.

SMAs can exist in the form of alloys with various chemical compositions, such as NiTi, copper-aluminium-nickel, copper-zinc-aluminium, and iron-manganese-silicon. However, NiTi alloys are considered the most useful and preferred type of SMAs. The first reason is because of their superior mechanical properties, such as the ability to recover from deformed strain, high ductility, and variable shape-memory properties that can be gained using a suitable heat treatment [15]. The second reason is their commercial availability compared with other types of SMAs, especially for applications with activation temperatures below 100 °C [15]. In general, NiTi alloys can be called Nitinol, which refers to their composition as well as the laboratory where they were first discovered (Naval Ordinance Laboratory) [16]. These unique and distinct properties of SMAs have promoted their potential use in building smart structures that can react and adapt rapidly to changes in environmental or working conditions [17].

The outstanding capability of SMA actuators in generating very large recovery forces from pre-compressed SMA rods in the field of rock-splitting [7, 11, 18, 19] has made their implementation in large-force AD applications an emerging and promising field of research. Most AD applications using SMA actuators are concerned with disassembling electronic products or products that require small disassembly forces [15].

To implement an SMA actuator in AD, it must be implanted in the product structure during the manufacturing phase. The disassembly process can be started using a single or combination of triggers that initiate the simultaneous disassembly of the product components. This is conducted without any direct physical contact between the disassembly tool and the components of the product [20], thus allowing the high-speed, low-cost, and non-destructive disassembly of product components that enables their future reuse [21], which will be shown in Section 4.

Great importance is currently given to the possibility of generating large forces from the SMA actuator. A deformed SMA rod can generate large recovery stresses (400–480 MPa) by restricting their transformation during heating [15, 18]. To enhance this property, certain parameters must be considered, such as compressive strain, activation temperature, activation time, and SMA cross-sectional area [22, 23, 24].

SMAs can recover large strains, i.e. up to 6% or 8% strains under ideal conditions [24, 25]. However, it is recommended that the strain used be limited to 3–4% to increase the expected lifetime of SMA actuators [24, 25]. Nishida [19] stated that the value of the recovery force decreases with increasing strain used above a certain limit. Thus, the strain used can be considered as the most important factor affecting the expected lifetime of SMA elements and the value of generated forces.

E. A. Williams [25] stated that the amount of the generated force is proportional to the SMA diameter. Thus, to generate large forces, large diameters must be implemented. The generated force also increases with increasing activation temperature [26]. However, to ensure the long lifetime of the SMA element, overheating and exceeding the recommended strain value must be avoided [13]. Chiodo [22] stated that the long activation time decreased the generated force. As a result, it was recommended that the heating process be conducted for less than 1 min to ensure the generation of the maximum possible recovery force [27].

The present research investigates the possibility of implementing SMA actuators in large-force AD applications. This investigation was conducted in three consecutive phases. The first phase includes studying the effect of different compressive strains on the generated recovery forces and the strain-hardening induced in the material to generate the maximum possible recovery force without affecting the lifetime of the SMA element, in addition to allowing its repetitive use. The second phase includes estimating the optimum compressive strain value that can generate the maximum recovery force with the least amount of residual strains induced in the material. To the best of the authors' knowledge, most of the experimental work in the field of compression applications of SMA actuators recommend a strain range rather than a specific strain value. The third phase presents an example to evaluate the possible implementation of the SMA actuator in large force AD applications.

2. Experimental procedures

In this phase, one SMA rod with a diameter of 10 mm and length of 100 mm was used to study the effect of different compressive strains on the generated recovery force and the induced strain hardening in the material. The rod was purchased from Kellogg's Research Labs [28] with a chemical composition of 55.74 wt.% Ni and 44.21 wt.% Ti, and transition temperatures of 35 °C and 45 °C as the austinite start and austenite finish temperature, respectively.

The emergence of the SME in the purchased rod was checked before starting the experimental investigation. A custom heater was designed to provide the necessary heating medium for the SMA rod. Finally, the compression of the SMA rod and the measurements of the recovery force were conducted using an electronic universal testing machine (UTM) controlled by PC-model WDW-100D, available at the materials testing lab.

2.1. Preparation of the SMA sample

Two samples were prepared. The first sample (Sample "E") was used to ensure the existence of the SME property, which is responsible for the ability of the SMA element to recover its original shape. The second sample (Sample "X") from the rod was subjected to compression testing. The length to the diameter ratios (L:d) of samples "E″ and "X" were maintained at ≤ 2 to prevent buckling during compression testing [17]. All the samples were prepared using a wire-cutting technique to prevent the exposure of the rods to elevated temperatures during the cutting process. The 10 mm diameter samples (sample "E "and "X") were cut to a length of 20 mm.

The existance of the SME was ensured by cutting sample "E" into thin slices that could be bent by hand using the wire-cutting technique. These slices were bent and placed in a hot water bath. It was observed that all the slices recovered their original straight shape, indicating the SME in the purchased rods. Figure 1 A and B illustrates the effect of the hot water bath on the deformed slices.

The second sample "X" was compressed several times at a constant strain rate of 0.05 s^{-1}. All compression testing was conducted at a room temperature of 20 °C. Compression strains with a step of approximately 0.25% were used to study the effect of different compressive strains on the generated recovery force and the induced strain hardening in the material.

2.2. Preparation of the SMA heater

In general, nitinol is characterised by its high resistivity that allows heating of the SMA element by passing an electric current directly through it [3, 29]. However, this technique is not recommended for heating SMA elements that will undergo a compression process. A compressed SMA element requires a high current to reach its austenite finish temperature, which cannot be supplied by the passage of a direct electric current. In this case, the preferred method is heating using an external heat source; for example, placing the SMA element in a medium heated to the desired temperature [24]. Thus, the SMA rods used throughout this research were not heated through the direct passage of electric current. Instead, a special custom heater was developed to supply the necessary heating as fast as possible to decrease the

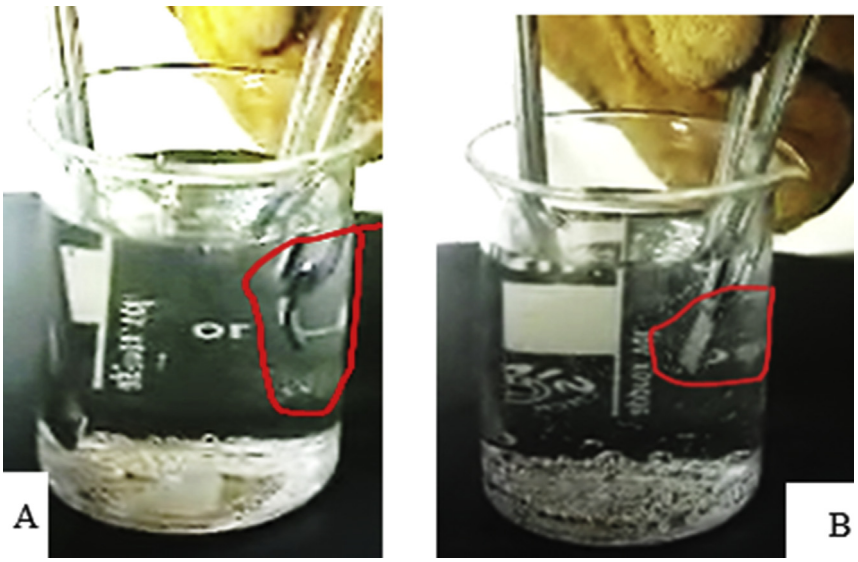

Figure 1. "A" represents the deformed slice of sample "E" after its insertion in a water bath. "B" indicates that the deformed slice was restored to its original shape owing to increasing the temperature of the water bath above the austenite finish temperature.

activation time needed to generate the recovery forces; slow heating rates reduce the effect of the recovery force [22].

The custom heater was designed to complete the heating process within a short time to ensure the generation of the maximum possible recovery force. In general, the heating time is affected only by the SMA cross-sectional area and electric current used; the SMA length has no impact [30]. Previous studies on the generation of large forces to split rocks recommended that the heating process be conducted in less than 1 min [7, 11, 18, 19]. Thus, the custom heater was designed to conduct the heating process in less than 1 min.

The experiments were conducted to select the appropriate heating wire dimensions, type of DC power supply, and type of electrical insulator that allows the conduction of heat between the SMA rod and heating coil as well as to select the suitable electric insulation between the different turns of the heating coil. To decrease the heating time, two different Ni-chrome wire diameters (0.9 and 0.7 mm) and power supplies were applied. Each wire was heated by passing an electric current using the following power supply values: 19V-3.42A, 24V-3A, and 24V-10A, respectively. The required heating time (approximately 50 s) was achieved using a 0.7 mm Ni-chrome wire and a 24V-10A power supply.

To select the necessary electric insulation between the SMA rod and heating coil while allowing the conduction of heat, several insulation methods were tested. These include wrapping the SMA rod with a brown-coated fiberglass fabric with silicone adhesive electric insulating tape; inserting the coil into a silicone-coated fiberglass sleeve; and inserting the SMA rod into a ceramic tube while winding the coil around the tube. Among these, inserting the rod into the ceramic tube was found to be the most effective insulation technique. Both the tape and sleeve could not withstand the high temperatures that evolved during the passage of the current through the wire. As for the required electric insulation between the different turns of the coil, a grey rubber silicone paste was used that can withstand temperatures of up to 350 °C. The operating temperature was not increased by more than 50 °C above the manufacturer's recommended austenite finish temperature (45 °C), as mentioned in Section 1. The final developed heater consisted of a ceramic tube, nichrome coil with a 0.7 mm wire diameter, rubber silicone paste, and 24V-10A DC power supply. Figure 2 presents a detailed illustration of the different components of the developed custom heater.

2.3. Investigation of the compressive strain effect on the generated recovery force

In this section, an experimental investigation of the behaviour of the SMA rod upon exposure to different compressive strains was conducted. During this investigation, the compressive strain values were maintained below 5%. This decision was based on T. Fukuta et al. [14], which proved that a 5% strain is not recommended for SMAs that will be subjected to compression testing. The exposure of the SMA element to large strains increases the amount of strain hardening induced in the material and the residual strain when the material is unloaded [17]. It was mentioned in the Introduction that a strain range of 3–4% is the most commonly used for different SMA applications. However, for most SMA compression applications, it was observed that the compressive strain should be maintained at 2–3% [7, 11, 18, 19, 31]. Thus, this section studies the effects of compressive strains from 2% to 4% on the generated recovery force to determine the optimum compressive strain value that can generate the maximum recovery force with the least amount of residual strain induced in the material.

During testing, sample "X" was compressed using the recommended strain values, inserted into the developed heater and placed between the two jaws of the UTM, and then allowed to increase its temperature freely above its austenite finish temperature (45 °C) to obtain the maximum

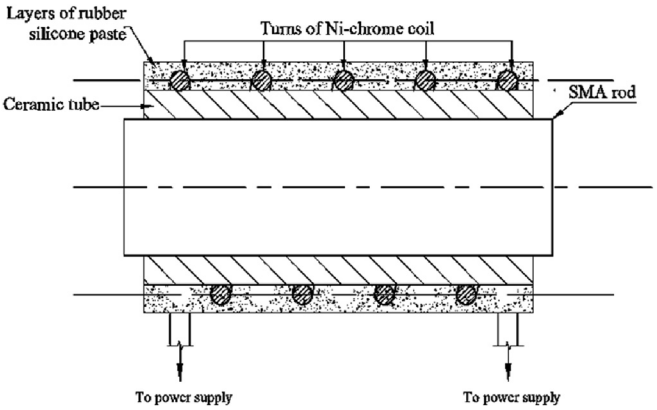

Figure 2. Detailed drawing for the components of the developed custom heater.

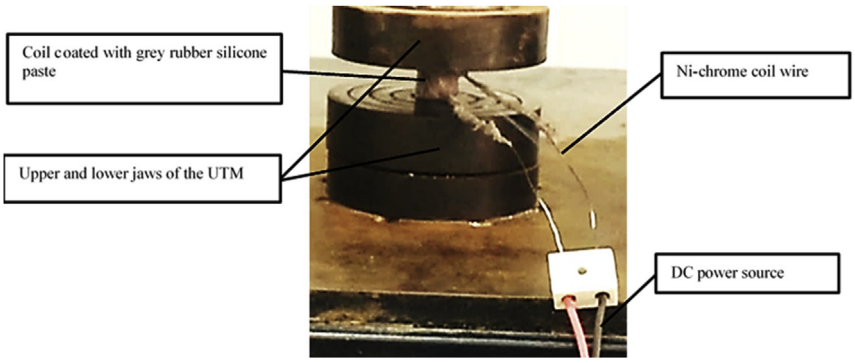

Figure 3. Custom heater of the SMA rod connected to a power supply and placed between the two jaws of the UTM during testing.

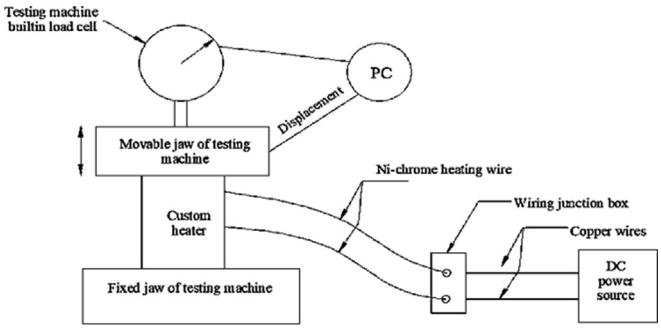

Figure 4. Schematic layout for the custom heater of the SMA rod connected to a power supply and placed between the two jaws of the UTM during testing.

possible recovery force. Overheating in a hot water bath was conducted at a temperature 50 °C above the recommended austenite finish temperature (45 °C) to relieve any residual strains that might have been induced in the material, and ensure that the sample can withstand repetitive usage. Figure 3 shows the arrangement of the SMA inserted into the heater and placed between two jaws of the UTM during the heating and measurement of the recovery force. In all the experiments, the resulting recovery force and residual induced strains were recorded. The compression process and recovery force measurements were conducted on the UTM at the materials testing lab. Figure 4 presents the simplified layout of the experimental setup.

2.4. Results and discussion

During testing, sample "X" was compressed at different compressive strain values of 2–4%, with a step of approximately 0.25%, to study the effects of repeated loading on the generated recovery force and residual strains induced in the material. First, the effect of large compressive strain on the behaviour of the SMA element was investigated by compressing the sample with a large strain of 4.3% and 4%. When the compressed sample was heated to a temperature higher than its austenite finish temperature, the maximum recovery forces of 37.2 kN and 32.95 kN were obtained in 39 s and 55 s, respectively. However, when cooled down to room temperature, the generated forces decreased to 18.6 kN and 18 kN, respectively. The occurrence of the residual recovery force

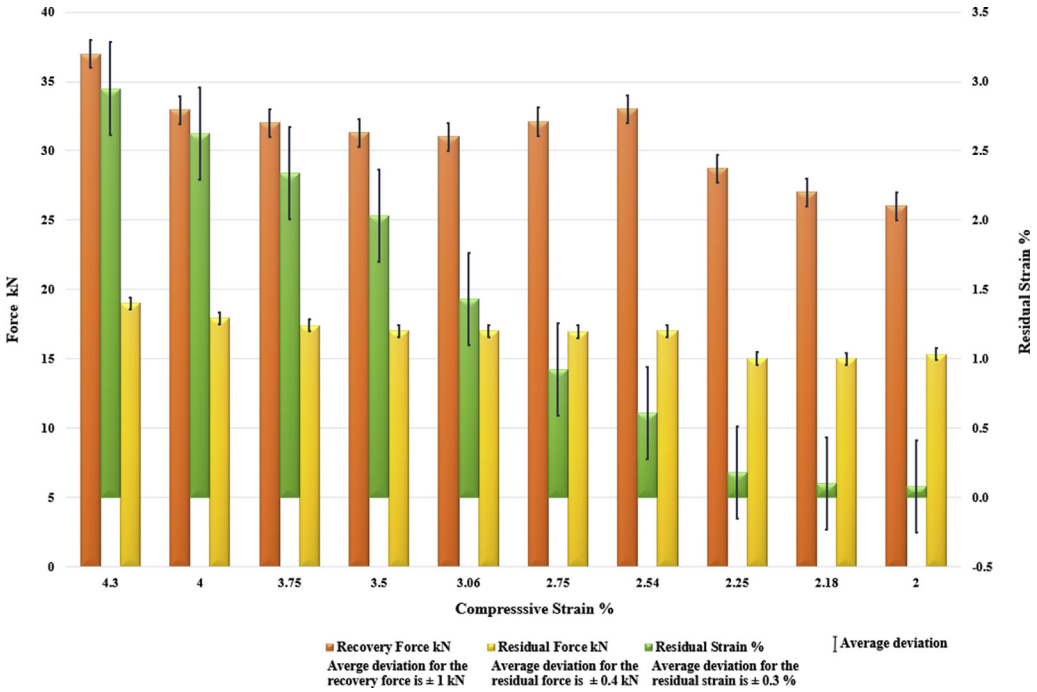

Figure 5. Effect of the compressive strain on the recovery force, the residual force, and the induced residual strains upon heating above the austenite finish temperature.

Table 1. Specifications of the Morse rod and spindle sleeve.

Type of Morse	MT2
Material of Morse rod and its spindle sleeve	Mild Steel (St.37)
Young's modulus of elasticity	210 GPa
Coefficient of static friction	0.1
Taper angle	1.45°
Tolerance deviation for MT2 [34]	±0.011 mm
Maximum interference between the Morse rod and its spindle sleeve	0.011 mm
Large Morse rod diameter	17.78 mm
Small Morse rod diameter	14.9 mm
Outer spindle sleeve diameter	34 mm
Length of contact	59 mm

was explained by Loughlan [32], i.e. this behaviour was attributed to the effect of the working temperature cycle, which prevented the complete formation of the martensite phase upon cooling down, as the temperature cycle is above the stressed martensite start temperature. In addition, it was observed that strain hardening was induced in the material because the sample did not recover 100% of its original length. The residual strain values were calculated as 2.95% and 2.6%, respectively, using Eq. (1) [33]:

$$\text{Residual Strain } \% = \Delta L/L \tag{1}$$

where:

ΔL: Represents the change in sample length upon heating.

L: Represents the original length of the sample before compression.

Owing to the high percentage of residual strains induced in the sample from the previous experiment, the required heating temperature in subsequent experiments is expected to be much higher than 45 °C, unlike the first set of experiments (maximum force was generated at 48 °C), to ensure both the maximum recovery of the compressed length and force generation. However, this temperature increase must be monitored to prevent sample damage. To relieve the effect of any residual strain induced in the sample from the previous experiments, it must be overheated to 50 °C above its austenite finish temperature after each heating-cooling cycle so that it can be subjected to repeated loading without affecting its performance.

To study the sample behaviour corresponding to the effect of repeated loading, a second set of experiments were conducted by compressing the sample using a strain range of 3–3.75%. Upon heating, the maximum generated force was less than that obtained from the previous experiment. The maximum generated force was 32 kN in 57 s at 83 °C. Upon cooling down to room temperature, the force and residual strain were reduced to 17.4 kN and 2.34%, respectively.

A third set of experiments was conducted to investigate whether using lower compressive strains can further reduce the amount of strain hardening induced in the material by reducing the amount of the induced residual strains. The sample was compressed using a strain range of 2–2.75%. Upon heating to 117 °C, the maximum recovery force generated was 33.43 kN at a strain of 2.54% in 50 s. Upon cooling down to room temperature, further improvement was observed in the residual strain, which decreased to 0.61%. Thus, the strain hardening induced in the material decreased, increasing its expected lifetime.

From the first set of experiments, it was observed that by using lower compressive strain values, the induced residual strains decreased, which improved the lifetime of the SMA element upon repeated loading. Figure 5 shows the effect of different compressive strains on the generated recovery forces, residual forces, and residual strains.

From Figure 5, it can be observed that subjecting the sample to very large strain values negatively affects its performance upon repeated loading by inducing large a amount of residual strains, despite of the large recovery forces generated; this increases the amount of strain hardening and reduces the expected lifetime under repeated usage. It is also observed that the strain range of 2–3% is consistent with the behaviour of SMA elements under compression loading, where the value of the recovery force increased with increasing compressive strain and decreased with when the strain increases beyond a specific value [19]. The strain ranges from 3–4% is consistent with the general behaviour of SMAs, the recovery forces increased with increasing strain. However, the behaviour of the SMA sample in this strain range for compression loading was not preferred as it increased the amount of residual strains induced in the materials, thus significantly decreasing its expected lifetime. Thus, 2.54% can be considered the optimum strain value to generate the maximum possible force with a reasonable amount of residual strain.

3. Practical case study for using SMA actuator in large force active disassembly application

A test rig was built to investigate the potential implementation of AD in extracting the Morse of a twist drill holder from its spindle sleeve with a Morse number of 2 (MT 2). A lab simulation was built using a rod with an external Morse taper and an internal Morse taper sleeve. The specifications of the Morse rod and sleeve are listed in Table 1.

The rod and the sleeve were press-fitted into each other using the UTM. The effect of the forces generated during the drilling operations must be considered to ensure that the fit force used can withstand the large thrust force required to feed the drill into the workpiece, and that the required cutting torque will not loosen the rod from its spindle. In other words, the required press-fit force and cutting torque must be estimated according to the cutting conditions of the drilling operation. A twist drill was assumed to drill a 22 mm diameter hole in a workpiece under the working conditions listed in Table 2.

The force required to press-fit the rod into its sleeve can be estimated based on the thrust force required to feed the drill into the workpiece. The required thrust feed force and cutting torque were estimated using Eqs. (2) and (3) [35]:

$$F_a = 4.448.\left[2.K.f^{0.8}.d^{0.8}.B + K.d^2.E\right] \quad N \tag{2}$$

$$T_c = 0.113.\left[K.f^{0.8}.d^{1.8}.A\right] \quad N.m \tag{3}$$

where:

K: Work material constant, 24000

f: Feed factor, $f^{0.8} = 0.007$,

d: Drill diameter factor, $d^{0.8} = 0.89$, $d^{1.8} = 0.77$, $d^2 = 0.751$.

Table 2. Drilling operation working conditions.

Workpiece material	Steel with 200 BHN
Spindle speed	350 rpm
Feed rate	0.05 mm/rev.

Figure 6. Experimental setup to simulate the implementation of AD during the extraction of a Morse rod from its sleeve.

The required feed thrust force was estimated as approximately 4.2 kN, while the required cutting torque was estimated to be 16 kN.mm. To prevent the slippage of the Morse rod from its sleeve, the force used to press-fit them into each other must be > 4.2 kN, while the holding torque must be > 16 kN.mm. The Morse rod was press-fitted into its sleeve using a force of 15 kN. To validate whether the actuator used in Section 2.3 can generate the required recovery forces to extract the Morse from its sleeve, a theoretical model was built to estimate the required Morse extraction force (F_p) and holding torque (T) using Eqs. (4), (5), and (6) [36, 37, 38]:

$$F_p = P_c.S.(\mu - \mathrm{Tan}\theta) \quad N \tag{4}$$

$$T = \mu.\ P_c\ .2.\Pi.\ r_1(z).\ L_c\cos\theta \quad N.mm \tag{5}$$

$$P_c = \frac{E.\delta.\left[r_2^2 - r_1^2(z)\right]\cos\theta}{2.r_1(z).r_2^2} \quad MPa \tag{6}$$

where:

F_p: Required removal force, N
P_c: Contact pressure along tapered surfaces, MPa
S: Mean surface area of tapered surface, $S = \Pi.\frac{(D_L+D_s)}{2}.L_c$, mm^2
D_L: Large diameter of Morse, mm
μ: Coefficient of friction between Morse taper and spindle
D_s: Small diameter of Morse, mm
z: Depth of insertion, mm
ɵ: Taper angle, approximately 1.45°
r_{ss}: Small radius of spindle, mm
E: Young's modulus of elasticity, mm
r_2: Outer radius of spindle, mm
δ: Initial interference, mm
Lc: Length of contact between the Morse ad its sleeve, mm
$r_1(z)$: Outer radius of Morse in terms of depth of insertion, = $r_{ss}+(L_c\cos\theta$ - z) $\tan\theta$ mm

The force required to extract the Morse rod from its sleeve was estimated as 16 kN, while the holding torque that prevents the rotation of the Morse rod relative to its sleeve was estimated as 23 kN.mm. Comparison of these values with the results obtained from Section 2.3 show that the SMA actuator can generate sufficiently large forces to extract the Morse rod from its sleeve.

The lab simulation was conducted by press-fitting the Morse rod into its sleeve using a force of 15 kN. The SMA rod has a 10 mm diameter, 20 mm length, and was compressed at a strain of 2.54%. The heater described in Section 2.2 was used to provide the necessary heating medium to activate the SMA. A slight modification was made on the heater by replacing the insulation technique with a more stable one. The silicone paste was replaced by a refractory cement, which is more stable at elevated temperatures and capable of withstanding repetitive usage, unlike the silicone paste whose layers required changing after two activations. The long wires of the heating coil that were exposed to air were insulted using thermal beads. Figure 6 shows the experimental setup for the Morse rod-sleeve assembly.

When the SMA rod was heated to above its recommended austenite finish temperature (45 °C), it successfully generated a recovery force large enough to release the Morse rod from its sleeve in 48 s. Figure 7 illustrates the different phases of the Morse-sleeve assembly separation process using AD. To emphasise that the same extraction process can be repeated several times, the Morse rod was assembled with its sleeve using the same press-fit force, while the SMA rod used was compressed using compressive strains of 2% and 3%. The extraction process was successfully conducted at each compressive strain. However, it was observed

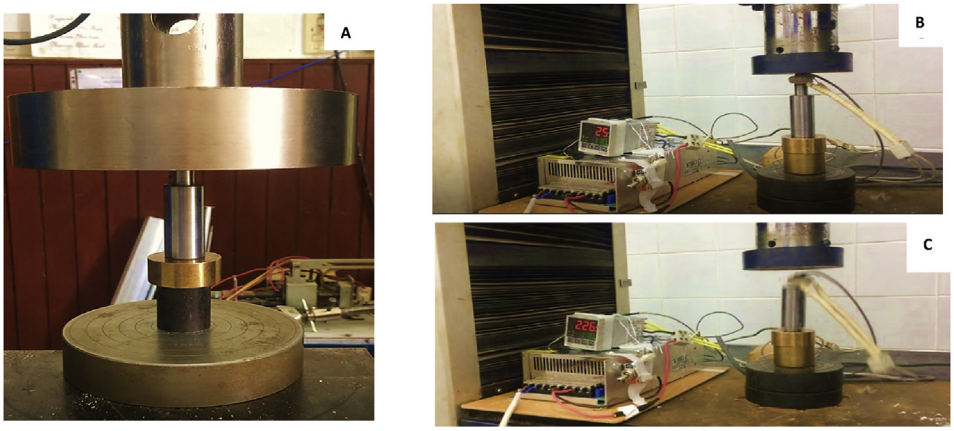

Figure 7. Different phases of the More-sleeve AD process where (A) shows the assembly process of the Morse rod into its sleeve using the press force generated from the UTM, (B) shows the step up before the SMA rod activation, and (C) shows that the activation process has been started and the Morse rod has separated from its sleeve.

that the required activation temperature increased with increasing compressive strain. The required activation time also increased with increasing compressive strain from 43 to 56 s. This was attributed to the increased amount of strain hardening induced in the material upon the repeated usage of the SMA rod above the recommended compressive strain value.

4. Conclusions

In this research, the authors studied the behaviour of the same SMA rod under the effects of the repeated compressive load, generated recovery force, and amount of residual strain induced in the material. It was observed that for SMA elements subjected to repetitive compressive loading, the compressive strain should be maintained at 2.54% to generate a large recovery force with the least amount of residual strain induced in the material. This increases the expected lifetime of the SMA element despite repeated usage.

The compressive strain can be increased to over 3% only if the SMA element is used once to generate extremely large forces without the possibility of repeated usage. This is because high strain values increase the amount of induced strain hardening in the material, which cannot be relieved by overheating above the austenite finish temperature. Thus, the generated recovery forces deteriorate significantly, reducing the expected lifetime of the SMA element.

The authors also investigated the possible implementation of the AD concept in applications that require a large disassembly force. A lab simulation was conducted in which the AD concept was used to separate a Morse rod from its sleeve for a drilling process. The SMA actuator successfully generated the required force to disassemble the Morse rod-sleeve assembly, and the AD process was completed in 48 s.

Declarations

Author contribution statement

Hoda Abuzied: Conceived and designed the experiments; Performed the experiments; Analyzed and interpreted the data; Contributed reagents, materials, analysis tools or data; Wrote the paper.

Ayman Abbas, Mohamed Awad & Hesham Senbel: Contributed reagents, materials, analysis tools or data; Wrote the paper.

Funding statement

This research did not receive any specific grant from funding agencies in the public, commercial, or not-for-profit sectors.

Competing interest statement

The authors declare no conflict of interest.

Additional information

No additional information is available for this paper.

References

[1] Z. Yuefeng, Design of active disassembly snap-fit based on electrothermal stimulation method, Bio Technol. 10 (16) (2014) 9309–9312.
[2] J. Carrell, H.C. Zhang, D. Tate, H. Li, Review and future of active disassembly, Int. J. Sustain. Eng. 2 (4) (2009) 252–264.
[3] Y.R. Mathew, B.G. Babu, A real time experimental set up to analyse automatic actuation of a fire sprinkler using a shape memory alloy (nitinol), Trans. FAMENA XXXIX 3 (2015) 9–22.
[4] J. Chekotu, R. Groarke, K. O'Toole, D. Brabazon, Advances in selective laser melting of nitinol shape memory alloy Part Production, Materials (Basel) 12 (5) (2019) 809.
[5] S. Faroughi, H. Haddad Khodaparast, M.I. Friswell, S.H. Hosseini, A shape memory alloy rod element based on the co-rotational formulation for nonlinear static analysis of tensegrity structures, J. Intell. Mater. Syst. Struct. 28 (1) (2017) 35–46.
[6] N. Jones, D. Harrison, H. Hussein, E. Billett, J. Chiodo, Towards self-disassembling vehicles, J. Sustain. Prod. Des. 3 (2004) 59–74.
[7] O. Benafan, R.D. Noebe, T.J. Halsmer, Static rock splitters based on high temperature shape memory alloys for planetary explorations, Acta Astronaut. 118 (2016) 137–157.
[8] J.P. Oliveira, N. Schell, N. Zhou, L. Wood, O. Benafan, Laser welding of precipitation strengthened Ni-rich NiTiHf high temperature shape memory alloys: microstructure and mechanical properties, Mater. Des. 162 (2019) 229–234.
[9] A. Chakraborty, Design and Characterization of Self-Biasing NiTi Spring Actuator, 2016.
[10] Z. Guo, Y. Pan, L.B. Wee, H. Yu, Design and control of a novel compliant differential shape memory alloy actuator, Sensors Actuators, A Phys. 225 (April) (2015) 71–80.
[11] O. Benafan, R.D. Noebe, T.J. Halsmer, Shape memory alloy rock splitters (SMARS)— a non-explosive method for fracturing planetary rocklike materials and minerals, Nasa 218832 (July) (2015) 35.
[12] E. Henderson, D.H. Nash, W.M. Dempster, On the experimental testing of fine Nitinol wires for medical devices, J. Mech. Behav. Biomed. Mater. 4 (3) (2011) 261–268.
[13] J.M. Jani, M. Leary, A. Subic, M.A. Gibson, A review of shape memory alloy research, applications and opportunities, Mater. Des. J. 56 (4) (2014) 1078–1113.
[14] T. Fukuta, M. IIba, Y. Kitagawa, Y. Sakai, Experimental study on stress-strain property of shape memory alloy and its application to self-restoration of structural members, in: 13th Wordl Conf. Earthq. Eng., no. 610, 2004, pp. 1–9.
[15] H. Abuzied, H. Senbel, M. Awad, A. Abbas, A review of advances in design for disassembly with active disassembly applications, Eng. Sci. Technol. Int. J. 23 (3) (2020) 618–624.
[16] Intrinsic Devices Inc, 2017, pp. 1–7. http://www.intrinsicdevices.com/Shape_Memory_Alloy_Fasteners.pdf," *Web*.
[17] M.S. Alam, M.A. Youssef, M. Nehdi, Utilizing shape memory alloys to enhance the performance and safety of civil infrastructure: a review, Can. J. Civ. Eng. 34 (9) (2007) 1075–1086.
[18] E.P, I.S. Stefano Carosio, Donato Zangani, Application of shape memory alloys to rock splitting : a successful example of co-operation between space research and industry, in: Proc. 2nd Conf. Acad. Ind. Coop. Sp. Res. ,Graz, no. ESA SP-470, 2000, pp. 15–17.
[19] M. Nishida, K. Kaneko, T. Inaba, A. Hirata, K. Yamauchi, Static rock breaker using TiNi shape memory alloy, Mater. Sci. Forum 56–58 (1991) 711–716.
[20] D.C, J.R.D. Paul Vanegas, Jef R. Peeters, "Disassembly," *CIRP Encyclopedia of Production Engineering*, Springer, 2019, pp. 506–510.
[21] L. Sun, W.M. Huang, H.B. Lu, C.C. Wang, J.L. Zhang, Shape memory technology for active assembly/disassembly: fundamentals, techniques and example applications, Assem. Autom. 34 (1) (2014) 78–93.
[22] J. Chiodo, N. Jones, Smart materials use in active disassembly, Assem. Autom. 32 (1) (2012) 8–24.
[23] S.G. Shu, D.C. Lagoudas, D. Hughes, J.T. Wen, Modeling of a flexible beam actuated by shape memory alloy wires, Smart Mater. Struct. 6 (3) (1997) 265–277.
[24] A.R. Srinivasa, A. Rao, J.N. Reddy, Design of Shape Memory Alloy (SMA) Actuators, SPRINGER B. Springer Briefs in Applied sciences and Technology· Computational Mechanics, 2015.
[25] E.A. Williams, G. Shaw, M. Elahinia, Control of an automotive shape memory alloy mirror actuator, Mechatronics 20 (5) (2010) 527–534.
[26] Y. Agata, Transactions of the materials research society of Japan, Supercond. Surfaces Superlattices 19 (2013) ii.
[27] T. Maruyama, H. Kubo, Shape Memory and Superelastic Alloys , Technologies and Applications, Woodhead Publishing limited, 2011.
[28] Kelloggs research labs [Online]. Available: https://www.kelloggsresearchlabs.com/product/rods/.
[29] A. Singh, J. Singh, P. Verma, Automotive application of shape memory alloys, in: 15th International Conference on Recent Trends in Engineering, Applied Science and Management, 2018, pp. 198–204.
[30] L. Miková, S. Medvecká, B.M. Kelemen, F. Trebuňa, I. Virgala, Application of shape memory alloy (SMA) as actuator, Metalurgija 54 (1) (2015) 169–172.
[31] Inderjit Chopra, J. Sirohi, Smart Structures Theory, Cambridge University Press, 2013.
[32] Thin-Walled Structures Advances and Developments, in: J. Zaras, K. Kowal-Michalska, J. Rhodes (Eds.), Third International Conference on Thin-Walled Structures, first ed., 2001.
[33] M. Paridah, A. Moradbak, A. Mohamed, F. abdulwahab taiwo Owolabi, M. Asniza, S.H. Abdul Khalid, Development of faster SMA actuators, Intech i (tourism) (2017) 13.
[34] Interplant Standard-steel industry - Tapers Dimesions and Tolerances- ISI :1715-1973." , 1973, Swatantra Bharat Press, Dalhi.
[35] M.M. Barash, Tool and manufacturing engineers handbook, Machining 1 (5) (1983). Library of Congress Catalog No. 82-060312 ,Society of Manufacturing Engineers (SME) Copyright.
[36] P. Lekomtsev, P. Božek, A. Romanov, A. Abramov, I. Abramov, Y. Nikitin, Extracting load research of taper interference fit made of glass and ceramics parts using a servo press, Appl. Mech. Mater. 816 (September) (2015) 461–468.
[37] J.H. Kang, The research on tapered joint design for power transmission of 2MW wind turbine 4 (12) (2014) 46–52.
[38] A. Risitano, Mechanical Design, CRC Press-Taylor & Francis Group, 2011.